# Comparison between global phenomenological and microscopic optical potentials for proton as projectile below 100 MeV

LI Xiao-Hua(李小华)[1;1)] LIANG Chun-Tian(梁春恬)[2] CAI Chong-Hai(蔡崇海)[1;2)]

1 (Department of Physics, Nankai University, Tianjin 300071, China)
2 (Department of Physics, Tianjin Institute of Urban Construction, Tianjin 300384, China)

**Abstract** For 112 target nuclei (52 elements) with proton as projectile, we calculate the reaction cross sections and elastic scattering angular distributions, as well as the $\chi^2$ values for 16 kinds of proton optical model potentials: two sets of phenomenological global optical potentials and the microscopic optical potentials proposed by Shen et al for 14 sets of Skyrme force parameters: GS1-6, SBJS, SKM, SGI-II, SKa-b, SG0I-II. We find that for obtaining the proton microscopic optical potential based on the nuclear matter approach with Skyrme force, SGI, SKa and SKb are the three sets of optimal Skyrme force parameters.

**Key words** microscopic optical potential, Skyrme force parameter, elastic scattering angular distributions, reaction cross sections, $\chi^2$ value

**PACS** 24.10.Ht, 25.45.-z

## 1 Introduction

The optical model (OM) has a significant impact on many aspects of nuclear physics, and its importance has already been indicated in Ref. [1]. OM is the basis and starting point for all nuclear model calculations and also is one of the most important theoretical approaches in nuclear data evaluation and analysis. The optical potential parameters are the key to reproducing the experimental data, such as reaction cross sections, and elastic scattering angle distributions. The optical potentials can be divided into two classes: microscopic and phenomenological optical potentials. Usually, the phenomenological optical potentials are of Woods-Saxon form; and the microscopic optical potentials are constructed through two different approaches: One is the so-called nuclear matter approach[2, 3], the other one is nuclear structure approach[4, 5].

Over the past years, there have been several sets of phenomenological global nucleon optical potentials, two of which are very popular. One was obtained by Varner et al[6] in 1991 which is called CH89 and the other one was presented by Koning et al[7] in 2003; we call it the KD potential. Both of them contain many adjustable parameters related to the energy of the projectile and the numbers of protons and nucleons in the target nucleus. These parameters were obtained by fitting the experimental data. However, for those nuclei which have a lack of or are without experimental data, and especially for the nuclei which are far away from the beta-stability line, we can not with full confidence use it to predict proton reaction cross sections and elastic scattering angular distributions, because it has no solid theoretical basis.

In this work, we calculate the proton reaction cross sections and elastic scattering angular distributions using the microscopic optical potential based on the nuclear matter approach with Skyrme force parameters. By using the effective Skyrme force in nuclear matter approach, Shen et al[8] obtained the semi-microscopic nucleon optical potential which has an analytical formula and is suitable for a large amount of calculations in nuclear data evaluation and

Received 22 September 2008

1) E-mail: lixiaohua@mail.nankai.edu.cn
2) E-mail: haicai@nankai.edu.cn

analysis. Also we shall compare the microscopic optical potentials with the phenomenological global optical potentials. The $\chi^2$ represents the degree of agreement between the calculated values of the reaction and differential elastic cross sections and their experimental data. We compare the $\chi^2$ values calculated with two sets of phenomenological global optical potentials (CH89 and KD) for proton as projectile and those calculated with the proton microscopic optical potential[8] based on nuclear matter approach with 14 kinds of Skyrme force parameters GS1-6[9], SBJS[10], SKM[11], SGI-Ⅱ[12], SKa-b[13], and SG0I-Ⅱ[14] for many target nuclei. If we use the proton microscopic optical potential based on nuclear matter approach to calculate the reaction and differential elastic cross sections for those nuclei with plenty of experimental data, and obtain good theoretical results in agreement with the experimental values, we can confidently extend it to those nuclei without experimental data, because it has a reliable theoretical basis. Shen and co-workers[15—20] made a large amount of calculations of neutron cross sections and angular distributions for various target nuclei and obtained rather good results in accordance with the experimental data. They found that for neutron as projectile, GS2 is the best set of Skyrme force parameters to construct the microscopic optical potential and the next one is SKa. Recently, we constructed the deuteron optical potential using a folding model based on phenomenological and microscopic nucleon optical potentials[21]. We found that SKa and SKb are the two best sets of Skyrme force parameters for obtaining the nucleon microscopic optical potential to construct the deuteron optical potential with a folding model. In this work, we will find which set of Skyrme force parameters is the best one for constructing the proton microscopic optical potential based on the nuclear matter approach.

This paper is arranged as follows. Sec. 2 is devoted to calculation and comparison of $\chi^2$ values, Sec. 3 gives the results and discussion. Finally, a summary is given in Sec. 4.

## 2 Calculation and comparison of $\chi^2$ values

In our calculations, two sets of phenomenological global proton optical potential parameters are taken from Refs. [6, 7], and 14 sets of Skyrme force parameters used in the calculation of proton microscopic optical potential are taken from Refs. [9—14].

For a certain nuclide, $\chi^2$ represents the deviation of the calculated values from the experimental data, which is defined as follows:

$$\chi^2 = \frac{1}{W_{\rm non}+W_{\rm el}}\left[\frac{W_{\rm non}}{N_{\rm non}}\sum_{i=1}^{N_{\rm non}}\left(\frac{\sigma^{\rm th}_{{\rm non},i}-\sigma^{\rm exp}_{{\rm non},i}}{\Delta\sigma^{\rm exp}_{{\rm non},i}}\right)^2+\frac{W_{\rm el}}{N_{\rm el}}\sum_{i=1}^{N_{\rm el}}\frac{1}{N_i}\sum_{j=1}^{N_i}\left(\frac{\sigma^{\rm th}_{\rm el}(i,j)-\sigma^{\rm exp}_{\rm el}(i,j)}{\Delta\sigma^{\rm exp}_{\rm el}(i,j)}\right)^2\right], \quad (1)$$

where $\sigma^{\rm th}_{\rm el}(i,j)$ and $\sigma^{\rm exp}_{\rm el}(i,j)$ are the theoretical and experimental elastic differential cross sections at the $j$-th angle with the $i$-th incidence energy, respectively. The subscript el means the data are for the elastic scattering angular distribution. $\Delta\sigma^{\rm exp}_{\rm el}(i,j)$ is the error of corresponding experimental data. $N_i$ is the number of angles for the $i$-th incidence energy. $N_{\rm el}$ is the number of incident energy points of elastic scattering angular distribution for a given target nucleus. $\sigma^{\rm th}_{{\rm non},i}$ and $\sigma^{\rm exp}_{{\rm non},i}$ are the theoretical and experimental reaction (or nonelastic) cross sections at the $i$-th incidence energy, respectively. The subscript non means the data are for the reaction cross sections. $\Delta\sigma^{\rm exp}_{{\rm non},i}$ is the error of corresponding experimental data. $N_{\rm non}$ is the number of incident energy points of reaction cross sections for a given target nucleus. The $W_{\rm el}$ and $W_{\rm non}$ are the weight of angular distribution of elastic scattering and reaction cross sections, respectively. As for the weights of $W_{\rm el}$ and $W_{\rm non}$, we believe that the experimental data of all nuclei are equally reliable. Considering the experimental data of angular distribution of elastic scattering are much more than those of reaction cross sections, in this work, we let $W_{\rm el}$=1.0 and $W_{\rm non}$=0.1 for all nuclei as in Ref. [22]. In order to have the same standard to determine the deviation of calculated values from experimental data, we set up the data errors as 5% of the experimental values of $\sigma_{\rm el}$ and $\sigma_{\rm non}$ for all target nuclei when we calculate the $\chi^2$, which are shown in Table 2, 3. The method of taking the errors as the same percentages of the experimental values is equivalent to the experimental values themselves taken as weights in calculation of the $\chi^2$ values, which is of benefit to find the best one from many sets of existing global optical potentials.

Our theoretical calculation is carried out in the non-relativistic frame; no consideration is given to the relativistic kinetics corrections because they are usually very small when $E \leqslant 200$ MeV (see Ref. [23]). All experimental data used in this work are taken from Ref. [22].

The analytical formula of Shen's semi-microscopic optical potential were driven from effective Skyrme force in nuclear matter approach[8], which are dependent on the density of nuclear matter. For finite nu-

clei, the local density approximation was introduced. That is to say, the nuclear density is a given function of nuclear radius, the optical potential is calculated at every given radius (corresponding to a certain nuclear density). So the calculated optical potential was also of radial distribution. Shen and co-workers[15—20] assumed that the densities of the neutrons and protons in a spherical nucleus have the same geometrical distributions and are expressed by Negele's[24] empirical formula, which is expressed as follows:

$$\rho_K(r)=\rho_{0K}\Big/\left[1.0+\exp\left(\frac{r-R}{a}\right)\right] \text{ for } K=N \text{ or } Z, \tag{2}$$

where

$$\rho_{0K}=\frac{3K}{4\pi R^3\left(1+\dfrac{\pi^2a^2}{R^2}\right)} \text{ for } K=N \text{ or } Z\,, \tag{3}$$

$$R=0.978\,A^{1/3}+0.0206\,A^{2/3},\quad a=0.54\,. \tag{4}$$

Table 1. Incident proton energy for every nucleus used in the calculations.

| nucleus | number of energy points | energy/MeV | nucleus | number of energy points | energy/MeV | nucleus | number of energy points | energy/MeV |
|---|---|---|---|---|---|---|---|---|
| $^{24}$Mg | 20 | 2.6—80 | $^{74}$Se | 1 | 64.8 | $^{144}$Sm | 1 | 65 |
| $^{25}$Mg | 2 | 9.1—17.5 | $^{78}$Se | 3 | 16—64.8 | $^{147}$Sm | 1 | 55 |
| $^{26}$Mg | 9 | 1.5—40 | $^{80}$Se | 3 | 16—64.8 | $^{148}$Sm | 3 | 16—66.5 |
| $^{27}$Al | 44 | 0.783—99.7 | $^{82}$Se | 2 | 16—64.8 | $^{149}$Sm | 1 | 55 |
| $^{28}$Si | 15 | 12.5—100 | $^{86}$Sr | 1 | 24.6 | $^{150}$Sm | 1 | 16 |
| $^{31}$P | 4 | 8—17.5 | $^{9}$Y8 | 4 | 21.1—65 | $^{152}$Sm | 2 | 16—65 |
| $^{32}$S | 7 | 15—25 | $^{90}$Zr | 24 | 5.574—100 | $^{160}$Gd | 1 | 65 |
| $^{37}$Cl | 1 | 35.2 | $^{91}$Zr | 21 | 14.5—49.35 | $^{159}$Tb | 9 | 20—98.7 |
| $^{40}$Ar | 18 | 14.1—65 | $^{92}$Zr | 7 | 12.7—49.35 | $^{164}$Dy | 1 | 65 |
| $^{39}$K | 1 | 35.2 | $^{94}$Zr | 5 | 12.7—49.35 | $^{165}$Ho | 3 | 16—99.1 |
| $^{40}$Ca | 48 | 9.86—100 | $^{96}$Zr | 3 | 22.5—60.8 | $^{166}$Er | 2 | 30—65 |
| $^{42}$Ca | 19 | 9—65 | $^{92}$Mo | 11 | 12.52—49.45 | $^{168}$Er | 1 | 65 |
| $^{44}$Ca | 22 | 9—65 | $^{94}$Mo | 5 | 12.52—49.45 | $^{169}$Tm | 2 | 55—99.3 |
| $^{48}$Ca | 20 | 9—65 | $^{96}$Mo | 6 | 12.52—49.45 | $^{172}$Yb | 1 | 16 |
| $^{45}$Sc | 3 | 35.2—99.2 | $^{98}$Mo | 4 | 12.52—65 | $^{174}$Yb | 2 | 16—65 |
| $^{46}$Ti | 4 | 50—65 | $^{103}$Rh | 2 | 10.13—17 | $^{176}$Yb | 3 | 16—65 |
| $^{48}$Ti | 11 | 16—65 | $^{104}$Pd | 7 | 10.25—35.4 | $^{178}$Hf | 1 | 65 |
| $^{50}$Ti | 7 | 14.15—65 | $^{106}$Pd | 2 | 22.3—51.93 | $^{180}$Hf | 1 | 65 |
| $^{51}$V | 13 | 7.5—99.1 | $^{106}$Cd | 1 | 22.3 | $^{181}$Ta | 15 | 9.7—98.3 |
| $^{50}$Cr | 2 | 51.93—65 | $^{108}$Cd | 1 | 22.3 | $^{182}$W | 1 | 65 |
| $^{52}$Cr | 6 | 10.77—65 | $^{110}$Cd | 2 | 20.4—22.3 | $^{183}$W | 1 | 55 |
| $^{53}$Cr | 8 | 10.13—12 | $^{111}$Cd | 1 | 14.235 | $^{184}$W | 2 | 16—65 |
| $^{54}$Cr | 1 | 65 | $^{113}$Cd | 1 | 14.24 | $^{186}$W | 1 | 16 |
| $^{54}$Fe | 36 | 3.73—65 | $^{115}$In | 20 | 3.009—20.4 | $^{188}$Os | 1 | 16 |
| $^{56}$Fe | 42 | 3.803—65 | $^{116}$Sn | 15 | 14.50—65.5 | $^{190}$Os | 1 | 16 |
| $^{57}$Fe | 11 | 6—60.8 | $^{118}$Sn | 11 | 14.50—83.2 | $^{192}$Os | 2 | 16—65 |
| $^{58}$Fe | 8 | 6—60.8 | $^{119}$Sn | 2 | 14.5—49.35 | $^{194}$Pt | 1 | 16 |
| $^{59}$Co | 30 | 3.88—98.5 | $^{120}$Sn | 23 | 9.7—65 | $^{198}$Pt | 1 | 16 |
| $^{58}$Ni | 37 | 7—81 | $^{122}$Sn | 9 | 20.4—49.35 | $^{197}$Au | 19 | 9.9—99.4 |
| $^{60}$Ni | 35 | 7—65 | $^{124}$Sn | 11 | 16—65.5 | $^{206}$Pb | 2 | 35—49.35 |
| $^{62}$Ni | 11 | 8.025—65 | $^{130}$Te | 5 | 9.5—14 | $^{207}$Pb | 1 | 12.98 |
| $^{64}$Ni | 12 | 9.6—65 | $^{134}$Ba | 1 | 16 | $^{208}$Pb | 33 | 5.5—100 |
| $^{63}$Cu | 27 | 7—50 | $^{136}$Ba | 1 | 16 | $^{209}$Bi | 8 | 10.76—78 |
| $^{65}$Cu | 25 | 7—50 | $^{138}$Ba | 1 | 16 | $^{232}$Th | 7 | 9.98—99.1 |
| $^{64}$Zn | 8 | 9.6—49.08 | $^{139}$La | 2 | 55—98.8 | $^{235}$U | 4 | 13.75—25 |
| $^{66}$Zn | 6 | 14.5—55.1 | $^{140}$Ce | 1 | 76 | $^{236}$U | 2 | 18—20 |
| $^{68}$Zn | 10 | 9.67—61.4 | $^{144}$Nd | 1 | 35 | $^{238}$U | 6 | 16—98.9 |
| $^{70}$Ge | 1 | 22.3 | | | | | | |

Table 2. $\chi^2_{ni}$ for every nuclide.

| nuclide | $\chi^2_{n\mathrm{CH89}}$ | $\chi^2_{n\mathrm{KD}}$ | $\chi^2_{n\mathrm{SG\,I}}$ | $\chi^2_{n\mathrm{SG\,II}}$ | $\chi^2_{n\mathrm{SKa}}$ | $\chi^2_{n\mathrm{SKb}}$ | $\chi^2_{n\mathrm{SG0\,I}}$ | $\chi^2_{n\mathrm{SG0\,II}}$ |
|---|---|---|---|---|---|---|---|---|
| $_{12}$Mg | 74.27 | 84.05 | 115.2 | 204.5 | 115.4 | 109.8 | 150.2 | 347.1 |
| $_{13}$Al | 30.94 | 29.96 | 90.43 | 201.5 | 83.77 | 80.42 | 103.2 | 299.9 |
| $_{14}$Si | 120.6 | 90.34 | 161.3 | 346.1 | 235.9 | 219.1 | 208.6 | 884.9 |
| $_{15}$P | 93.96 | 80.21 | 108.3 | 328.8 | 99.56 | 92.33 | 169.9 | 361.8 |
| $_{16}$S | 37.82 | 61.22 | 126.9 | 498.7 | 123.3 | 125.2 | 175.2 | 599.1 |
| $_{17}$Cl | 61.62 | 90.38 | 146.4 | 181.5 | 111.3 | 112.7 | 133.2 | 137.8 |
| $_{18}$Ar | 40.67 | 93.38 | 116.3 | 209.1 | 113.3 | 98.38 | 156.2 | 385.2 |
| $_{19}$K | 36.29 | 69.30 | 120.2 | 164.1 | 92.21 | 94.31 | 102.5 | 97.19 |
| $_{20}$Ca | 66.55 | 99.16 | 111.0 | 201.0 | 114.1 | 105.4 | 136.3 | 310.9 |
| $_{21}$Sc | 65.55 | 132.6 | 105.9 | 136.8 | 88.28 | 88.99 | 105.8 | 114.5 |
| $_{22}$Ti | 34.82 | 106.6 | 96.13 | 279.5 | 85.28 | 79.72 | 117.8 | 546.0 |
| $_{23}$V | 29.54 | 137.2 | 57.36 | 186.9 | 56.48 | 49.65 | 87.70 | 272.0 |
| $_{24}$Cr | 41.81 | 93.94 | 79.30 | 215.0 | 70.16 | 68.84 | 76.14 | 432.6 |
| $_{26}$Fe | 26.74 | 69.81 | 59.08 | 117.3 | 62.06 | 61.03 | 72.39 | 204.1 |
| $_{27}$Co | 19.36 | 38.98 | 52.60 | 101.0 | 50.66 | 47.26 | 63.65 | 133.5 |
| $_{28}$Ni | 33.83 | 83.68 | 84.66 | 190.2 | 77.66 | 77.89 | 109.4 | 317.1 |
| $_{29}$Cu | 18.41 | 69.12 | 47.62 | 103.8 | 43.81 | 51.81 | 56.83 | 209.9 |
| $_{30}$Zn | 70.77 | 214.5 | 109.7 | 178.1 | 127.8 | 122.7 | 147.2 | 438.7 |
| $_{32}$Ge | 65.18 | 640.5 | 249.6 | 469.3 | 278.2 | 262.9 | 303.4 | 948.0 |
| $_{34}$Se | 121.0 | 426.6 | 108.2 | 454.9 | 109.1 | 108.6 | 105.6 | 1186. |
| $_{38}$Sr | 21.65 | 227.6 | 192.4 | 312.3 | 193.5 | 186.8 | 288.1 | 611.8 |
| $_{39}$Y | 223.1 | 198.8 | 288.8 | 343.1 | 344.0 | 334.8 | 216.6 | 2863. |
| $_{40}$Zr | 70.06 | 271.9 | 145.8 | 322.0 | 152.2 | 160.6 | 210.8 | 826.9 |
| $_{42}$Mo | 64.63 | 255.6 | 108.7 | 273.0 | 114.5 | 120.4 | 145.0 | 703.9 |
| $_{45}$Rh | 8.086 | 116.3 | 53.04 | 176.1 | 72.90 | 65.26 | 59.28 | 364.5 |
| $_{46}$Pd | 53.44 | 344.0 | 171.5 | 319.2 | 192.3 | 199.4 | 228.1 | 835.9 |
| $_{48}$Cd | 11.21 | 135.2 | 118.1 | 230.9 | 140.8 | 152.0 | 144.9 | 569.7 |
| $_{49}$In | 0.778 | 11.81 | 10.43 | 15.40 | 12.49 | 12.93 | 10.70 | 40.44 |
| $_{50}$Sn | 46.11 | 121.6 | 150.0 | 233.6 | 140.1 | 241.9 | 137.7 | 919.0 |
| $_{52}$Te | 73.25 | 45.95 | 161.9 | 142.8 | 255.0 | 106.7 | 244.5 | 214.6 |
| $_{56}$Ba | 4.172 | 59.69 | 407.7 | 63.29 | 358.7 | 764.2 | 132.1 | 263.1 |
| $_{57}$La | 71.54 | 208.9 | 85.19 | 99.86 | 80.24 | 85.73 | 135.4 | 376.6 |
| $_{58}$Ce | 255.0 | 278.2 | 99.42 | 65.54 | 113.3 | 107.7 | 127.2 | 76.18 |
| $_{60}$Nd | 78.33 | 179.9 | 501.0 | 877.2 | 479.3 | 544.3 | 803.1 | 2381. |
| $_{62}$Sm | 74.23 | 133.1 | 360.0 | 296.0 | 327.4 | 531.5 | 246.0 | 949.9 |
| $_{64}$Gd | 484.4 | 478.6 | 272.7 | 1169. | 258.5 | 235.8 | 277.9 | 4617. |
| $_{65}$Tb | 105.3 | 86.09 | 133.3 | 129.3 | 129.4 | 130.3 | 127.1 | 51.99 |
| $_{66}$Dy | 604.1 | 514.9 | 365.0 | 1372. | 339.6 | 318.5 | 336.1 | 5064. |
| $_{67}$Ho | 106.3 | 138.5 | 189.0 | 121.5 | 183.2 | 249.6 | 150.8 | 179.0 |
| $_{68}$Er | 370.1 | 481.4 | 753.2 | 1443. | 756.2 | 741.4 | 1005. | 4339. |
| $_{69}$Tm | 66.51 | 114.2 | 69.94 | 61.17 | 68.93 | 72.91 | 87.60 | 99.29 |
| $_{70}$Yb | 190.3 | 234.5 | 334.1 | 444.6 | 351.9 | 373.2 | 340.0 | 1603. |
| $_{72}$Hf | 285.3 | 227.3 | 234.1 | 1014. | 199.6 | 189.1 | 306.6 | 4233. |
| $_{73}$Ta | 460.5 | 214.2 | 330.9 | 491.5 | 301.8 | 285.1 | 420.7 | 1479. |
| $_{74}$W | 115.3 | 95.94 | 158.3 | 355.9 | 149.6 | 148.4 | 162.7 | 1200. |
| $_{76}$Os | 178.9 | 108.1 | 272.5 | 544.8 | 259.1 | 252.5 | 261.7 | 1624. |
| $_{78}$Pt | 54.37 | 29.44 | 256.5 | 90.05 | 278.8 | 258.9 | 215.1 | 299.0 |
| $_{79}$Au | 107.8 | 139.4 | 251.0 | 411.9 | 252.3 | 278.2 | 373.2 | 2805. |
| $_{82}$Pb | 172.0 | 189.4 | 354.6 | 390.4 | 357.2 | 410.8 | 397.1 | 1545. |
| $_{83}$Bi | 249.7 | 167.7 | 204.3 | 306.7 | 218.0 | 203.2 | 215.8 | 1184. |
| $_{90}$Th | 384.2 | 481.8 | 1108. | 1358. | 1093. | 1301. | 1466. | 7459. |
| $_{92}$U | 52.76 | 86.14 | 140.7 | 123.5 | 128.4 | 172.7 | 119.6 | 597.0 |

Table 3. $\chi^2_{ni}$ for every nuclide.

| nuclide | $\chi^2_{n\mathrm{GS1}}$ | $\chi^2_{n\mathrm{GS2}}$ | $\chi^2_{n\mathrm{GS3}}$ | $\chi^2_{n\mathrm{GS4}}$ | $\chi^2_{n\mathrm{GS5}}$ | $\chi^2_{n\mathrm{GS6}}$ | $\chi^2_{n\mathrm{SBJS}}$ | $\chi^2_{n\mathrm{SKM}}$ |
|---|---|---|---|---|---|---|---|---|
| $_{12}$Mg | 112.4 | 103.7 | 115.9 | 371.9 | 293.2 | 287.3 | 550.3 | 212.4 |
| $_{13}$Al | 67.31 | 52.30 | 67.05 | 197.0 | 185.5 | 196.0 | 430.3 | 200.9 |
| $_{14}$Si | 335.1 | 218.0 | 195.9 | 802.2 | 791.4 | 576.6 | 1791. | 359.3 |
| $_{15}$P | 49.78 | 51.33 | 84.89 | 251.9 | 263.2 | 349.6 | 491.6 | 331.5 |
| $_{16}$S | 41.52 | 44.33 | 81.64 | 337.8 | 387.2 | 502.6 | 676.2 | 473.1 |
| $_{17}$Cl | 164.8 | 155.1 | 125.0 | 127.7 | 94.64 | 119.4 | 141.7 | 181.5 |
| $_{18}$Ar | 134.3 | 105.2 | 101.6 | 355.7 | 293.8 | 232.9 | 404.9 | 207.8 |
| $_{19}$K | 86.37 | 73.33 | 65.22 | 88.11 | 56.55 | 89.75 | 121.3 | 162.6 |
| $_{20}$Ca | 176.4 | 142.3 | 110.5 | 418.5 | 364.5 | 214.8 | 320.9 | 200.1 |
| $_{21}$Sc | 155.9 | 135.8 | 100.1 | 148.1 | 117.5 | 107.4 | 113.6 | 137.3 |
| $_{22}$Ti | 61.27 | 67.83 | 95.68 | 144.0 | 149.5 | 157.6 | 282.4 | 269.8 |
| $_{23}$V | 34.24 | 49.19 | 64.45 | 129.5 | 119.0 | 124.3 | 183.7 | 184.1 |
| $_{24}$Cr | 47.26 | 49.00 | 69.84 | 112.4 | 120.8 | 110.4 | 223.4 | 208.3 |
| $_{26}$Fe | 73.84 | 92.29 | 97.60 | 115.8 | 116.7 | 101.6 | 164.0 | 117.3 |
| $_{27}$Co | 35.86 | 39.64 | 54.18 | 77.16 | 79.18 | 82.04 | 103.1 | 97.75 |
| $_{28}$Ni | 67.21 | 81.88 | 113.1 | 118.8 | 113.5 | 135.7 | 203.7 | 189.4 |
| $_{29}$Cu | 71.38 | 95.99 | 120.7 | 65.02 | 60.12 | 59.84 | 107.6 | 111.5 |
| $_{30}$Zn | 246.2 | 232.9 | 148.3 | 273.0 | 288.6 | 202.0 | 293.9 | 171.5 |
| $_{32}$Ge | 150.0 | 145.8 | 160.2 | 430.5 | 516.2 | 468.6 | 457.4 | 393.7 |
| $_{34}$Se | 117.0 | 139.4 | 126.2 | 206.2 | 214.6 | 159.0 | 458.2 | 416.6 |
| $_{38}$Sr | 217.7 | 212.1 | 226.3 | 310.8 | 339.7 | 387.3 | 441.5 | 293.1 |
| $_{39}$Y | 221.2 | 202.2 | 208.5 | 574.2 | 375.5 | 341.8 | 3618. | 348.8 |
| $_{40}$Zr | 284.4 | 354.9 | 333.7 | 280.4 | 250.2 | 226.1 | 439.9 | 312.5 |
| $_{42}$Mo | 186.5 | 204.3 | 152.7 | 202.5 | 194.0 | 173.3 | 311.6 | 254.8 |
| $_{45}$Rh | 116.9 | 126.2 | 107.5 | 159.2 | 153.3 | 58.53 | 78.61 | 171.9 |
| $_{46}$Pd | 336.0 | 361.6 | 277.3 | 307.8 | 288.7 | 240.2 | 329.2 | 302.5 |
| $_{48}$Cd | 256.1 | 287.4 | 193.8 | 229.9 | 203.8 | 141.7 | 183.7 | 225.9 |
| $_{49}$In | 21.09 | 22.95 | 14.13 | 16.16 | 15.02 | 9.722 | 11.31 | 15.39 |
| $_{50}$Sn | 291.6 | 340.6 | 204.7 | 168.4 | 191.2 | 151.5 | 547.8 | 230.8 |
| $_{52}$Te | 147.7 | 104.6 | 58.78 | 331.5 | 457.1 | 248.6 | 98.60 | 127.0 |
| $_{56}$Ba | 1689. | 2721. | 1392. | 92.26 | 109.2 | 130.7 | 58.49 | 75.68 |
| $_{57}$La | 201.8 | 209.1 | 159.1 | 119.5 | 94.68 | 118.3 | 194.3 | 97.13 |
| $_{58}$Ce | 168.1 | 168.6 | 162.9 | 157.1 | 205.2 | 137.7 | 103.2 | 62.44 |
| $_{60}$Nd | 666.1 | 832.7 | 900.6 | 720.2 | 609.2 | 854.0 | 1535. | 869.3 |
| $_{62}$Sm | 888.7 | 1466. | 1108. | 244.0 | 250.7 | 250.4 | 440.8 | 277.1 |
| $_{64}$Gd | 330.8 | 395.5 | 326.1 | 213.1 | 392.1 | 470.4 | 2775. | 1041. |
| $_{65}$Tb | 109.5 | 104.0 | 114.6 | 138.6 | 123.9 | 117.3 | 52.52 | 130.8 |
| $_{66}$Dy | 341.1 | 420.1 | 381.0 | 244.4 | 461.3 | 569.2 | 3139. | 1228. |
| $_{67}$Ho | 301.6 | 501.2 | 546.6 | 193.2 | 190.6 | 152.4 | 61.74 | 122.6 |
| $_{68}$Er | 949.3 | 1037. | 939.6 | 970.6 | 1032. | 1116. | 2759. | 1327. |
| $_{69}$Tm | 109.6 | 109.7 | 97.15 | 99.02 | 84.27 | 78.69 | 77.49 | 61.44 |
| $_{70}$Yb | 460.3 | 579.1 | 579.6 | 417.0 | 473.5 | 422.0 | 831.9 | 393.0 |
| $_{72}$Hf | 346.6 | 406.5 | 356.8 | 217.7 | 365.5 | 436.9 | 2359. | 910.4 |
| $_{73}$Ta | 191.3 | 280.3 | 524.0 | 273.3 | 584.8 | 708.3 | 1684. | 439.1 |
| $_{74}$W | 197.2 | 202.4 | 181.9 | 145.1 | 188.5 | 200.1 | 669.9 | 323.4 |
| $_{76}$Os | 256.3 | 277.8 | 315.7 | 228.0 | 337.2 | 344.2 | 903.6 | 487.9 |
| $_{78}$Pt | 337.1 | 280.4 | 268.5 | 260.8 | 367.1 | 276.7 | 84.41 | 85.17 |
| $_{79}$Au | 477.0 | 541.1 | 538.1 | 384.6 | 426.1 | 404.6 | 1456. | 403.2 |
| $_{82}$Pb | 471.7 | 584.9 | 523.4 | 363.0 | 363.5 | 403.2 | 809.7 | 388.6 |
| $_{83}$Bi | 199.8 | 232.9 | 219.4 | 182.0 | 285.2 | 280.9 | 864.1 | 280.0 |
| $_{90}$Th | 1532. | 1920. | 2053. | 1353. | 1091. | 1280. | 2629. | 1413. |
| $_{92}$U | 212.2 | 255.6 | 265.4 | 117.2 | 127.7 | 149.4 | 214.9 | 188.3 |

Table 4. The values of $\bar{\chi}_i^2$, $\langle\bar{\chi}_i^2\rangle$.

| $i=$ | CH89 | KD | SG Ⅰ | SG Ⅱ | SKa | SKb | SG0 Ⅰ | SG0 Ⅱ |
|---|---|---|---|---|---|---|---|---|
| $\bar{\chi}_i^2$ | 117.9 | 174.8 | 200.5 | 353.2 | 200.8 | 217.2 | 230.3 | 1127. |
| $\langle\bar{\chi}^2{}_i\rangle$ | 0.36356 | 0.66086 | 0.64968 | 1.10231 | 0.65139 | 0.67485 | 0.73543 | 2.65246 |
| $i=$ | GS1 | GS2 | GS3 | GS4 | GS5 | GS6 | SBJS | SKM |
| $\bar{\chi}_i^2$ | 283.5 | 342.7 | 304.4 | 278.6 | 293.4 | 291.5 | 717.0 | 336.8 |
| $\langle\bar{\chi}^2{}_i\rangle$ | 0.87494 | 0.99348 | 0.89053 | 0.98723 | 1.00726 | 0.93442 | 1.75111 | 1.07023 |

Table 5. The best three sets of Skyrme force for obtaining the proton microscopic optical potential based on nuclear matter approach.

| | $t_0$/ (MeV·fm$^3$) | $t_1$/ (MeV·fm$^5$) | $t_2$/ (MeV·fm$^5$) | $t_3$ | $t_4$/ (MeV·fm$^8$) | $x_0$ | $x_1$ | $x_2$ | $x_3$ | $x_4$ | $W_0$/ (MeV·fm$^5$) | $\alpha$ |
|---|---|---|---|---|---|---|---|---|---|---|---|---|
| SKa | −1602.78 | 570.88 | −67.70 | 8000 | 0 | −0.02 | 0 | 0 | −0.286 | 0 | 125 | 1/3 |
| SKb | −1602.78 | 570.88 | −67.70 | 8000 | 0 | −0.165 | 0 | 0 | −0.286 | 0 | 125 | 1/3 |
| SGI | −1603 | 515.9 | 84.5 | 8000 | 0 | −0.02 | 0 | 0 | 0.1381 | 0 | 115 | 1/3 |

In the above equations, $N$ and $Z$ are the numbers of neutron and proton in the target nuclei, respectively. $R$ and $a$ are the radius and diffusiveness parameters of the target, respectively.

In our recent work[21] and this work, we use the same nuclear density distribution as mentioned above. We think that as universal semi-microscopic optical potentials, we should not introduce any additional free parameters.

## 3 Results and discussion

In the test calculations, we find that if the incident energy is higher than 100 MeV, all the calculated $\chi^2$ values of the microscopic optical potential based on nuclear matter approach with Skyrme force parameters and of the global optical potential parameters obtained by Varner et al.[6] become very large. This can be understood easily. For the microscopic optical potential based on nuclear matter approach with Skyrme force, all of the Skyrme force parameters were obtained by fitting the basic properties of the nuclear matter and the ground states of many nuclei (of course they are valid only for the lower energy region); for the global optical potential CH89 obtained by Varner et al.[6], the databases for obtaining this set of parameters are in the energy region below 65 MeV. So in the following calculations we only choose experimental data below 100 MeV. Also the conclusions and remarks obtained by us later are valid only for the energy region below 100 MeV.

The target nuclei and the corresponding incident energies used in our calculations are shown in Table 1, and we use $\chi^2_{n\mathrm{KD}}$, $\chi^2_{n\mathrm{CH89}}$ to express the $\chi^2$ calculated with the global optical potential of Koning et al[7] and Varner et al[6] for the $n$-th element, the $\chi^2_{ni}$ for $i$= GS1-6, SBJS, SKM, SGI-Ⅱ, SKa-b, SG0I-Ⅱ (see Table 2, 3) to express the $\chi^2$ calculated with the microscopic optical potential corresponding to the Skyrme force parameters[9—14], respectively. The results are given in Table 2, 3. In the calculation of the proton microscopic optical potential, we use the analytical formula given by Shen et al[8].

In order to find the best one among the 14 kinds of proton microscopic optical potentials, we define

$$\bar{\chi}_i^2 = \frac{1}{N}\sum_{n=1}^{N}\chi^2_{ni} \quad \text{with} \quad i=\mathrm{KD,CH89,SBJS,}\\ \mathrm{SKM,SGI\text{-}Ⅱ,SKa\text{-}b,SG0I\text{-}Ⅱ}, \tag{5}$$

$$\bar{\chi}^2_{ni} = \frac{16\chi^2_{ni}}{\sum\limits_j \chi^2_{nj}} \quad \text{with} \quad i,j=\mathrm{KD,CH89,SBJS,}\\ \mathrm{SKM,SGI\text{-}Ⅱ,SKa\text{-}b,SG0I\text{-}Ⅱ}, \tag{6}$$

$$\langle\bar{\chi}_i^2\rangle = \frac{1}{N}\sum_{n=1}^{N}\bar{\chi}^2_{ni} \quad \text{with} \quad i=\mathrm{KD,CH89,SBJS,}\\ \mathrm{SKM,SGI\text{-}Ⅱ,SKa\text{-}b,SG0I\text{-}Ⅱ}, \tag{7}$$

where $N=52$ is the total number of target elements (see Tables 2, 3). For a given target element $n$, the $\bar{\chi}^2_{ni}$ defined in Eq. (6) is the relative $\chi^2$ of the $i$-th optical potential among the 16 kinds of optical potentials. For these 52 elements, $\bar{\chi}_i^2$ defined in Eq. (5) is the average value of $\chi^2$ of these 52 elements calculated using the $i$-th optical potential; $\langle\bar{\chi}_i^2\rangle$ defined in Eq. (7) is the average value of the relative $\chi^2$, and it is used to show which is the best one among the 14 kinds of proton microscopic optical potentials more clearly than $\bar{\chi}_i^2$. The values of these $\chi^2_{ni}$ are given in Tables 2, 3 and both the $\bar{\chi}_i^2$ and $\langle\bar{\chi}^2{}_i\rangle$ are given in Table 4.

From Table 2, we can see that except for $_{13}$Al, $_{14}$Si, $_{15}$P, $_{39}$Y, $_{52}$Te, $_{64}$Gd, $_{65}$Tb, $_{66}$Dy, $_{72}$Hf, $_{73}$Ta,

$_{74}$W, $_{76}$Os, $_{78}$Pt, $_{83}$Bi, the value of $\chi^2_{n\mathrm{CH89}}$ is always less than the corresponding $\chi^2_{n\mathrm{KD}}$ value because the global proton optical potential parameters of CH89 were obtained by fitting the experimental data for incident energies below 65 MeV, while the global proton optical potential parameters of KD were obtained by fitting the experimental data for incident energies below 200 MeV. Generally, these two sets of global proton optical potentials can basically reproduce the experimental data well. From Table 2, we can see that except for $_{32}$Ge, $_{39}$Y, $_{60}$Nd, $_{62}$Sm, $_{64}$Gd, $_{66}$Dy, $_{68}$Er, $_{70}$Yb, $_{72}$Hf, $_{73}$Ta, $_{76}$Os, $_{78}$Pt, $_{79}$Au, $_{82}$Pb, $_{83}$Bi, $_{90}$Th, the values of $\chi^2_{n\mathrm{SGI}}$ are less than 200; except for $_{14}$Si, $_{32}$Ge, $_{39}$Y, $_{52}$Te, $_{56}$Ba, $_{60}$Nd, $_{62}$Sm, $_{64}$Gd, $_{66}$Dy, $_{68}$Er, $_{70}$Yb, $_{73}$Ta, $_{74}$W, $_{76}$Os, $_{79}$Au, $_{82}$Pb, $_{83}$Bi, $_{90}$Th, the values of $\chi^2_{n\mathrm{SKa}}$ are less than 200; except for $_{14}$Si, $_{32}$Ge, $_{39}$Y, $_{50}$Sn, $_{56}$Ba, $_{60}$Nd, $_{62}$Sm, $_{64}$Gd, $_{66}$Dy, $_{68}$Er, $_{70}$Yb, $_{73}$Ta, $_{76}$Os, $_{78}$Pt, $_{79}$Au, $_{82}$Pb, $_{83}$Bi, the values of $\chi^2_{n\mathrm{SKb}}$ are less than 200. Many are less than 100.

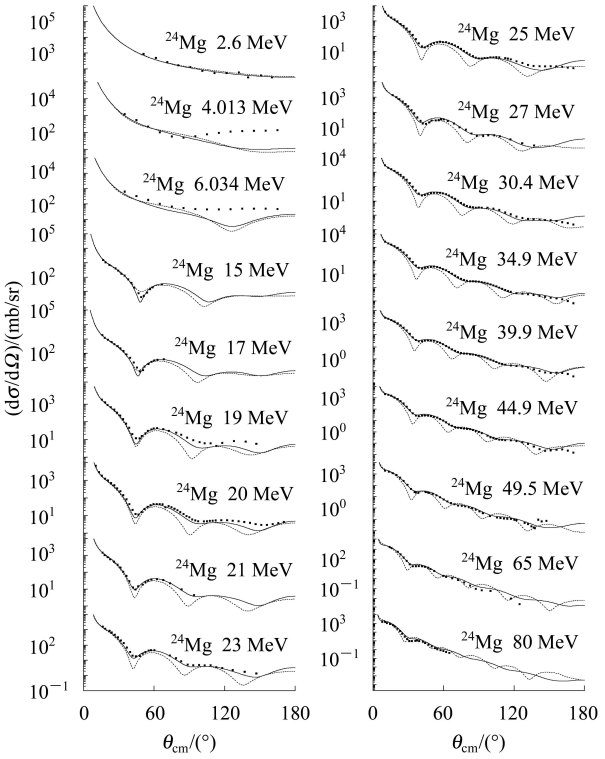


Fig. 1. Comparisons between the experimental angular distributions of elastic scattering in the center of mass frame for $^{24}$Mg and the calculated values from the global proton optical potential CH89 and the proton microscopic optical potential with Skyrme force parameter SKa. The black dots denote the experimental data, the solid lines represent the values of CH89, and the dashed lines correspond to the values of SKa. The experimental data are taken from Ref. [22], and the same symbols are used in Fig. 2.

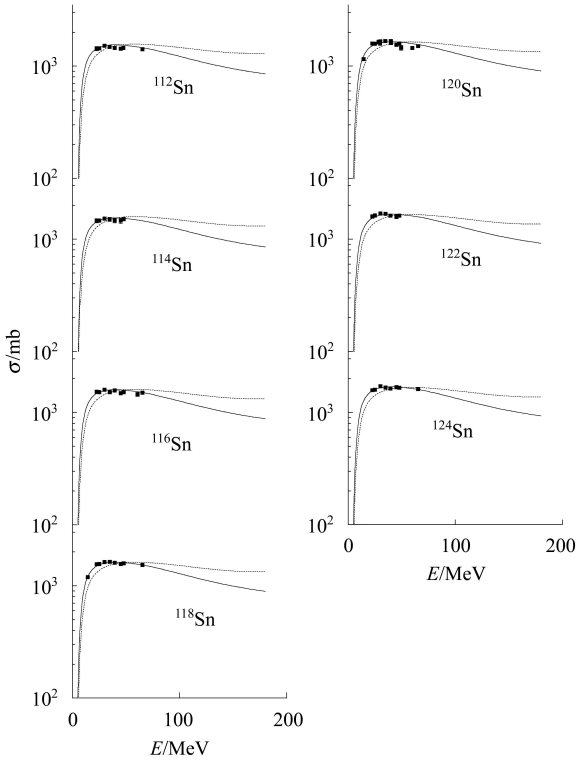


Fig. 2. Comparisons between the experimental reaction cross sections and the calculated values from the global proton optical potential CH89 and the proton microscopic optical potential with Skyrme force parameter SKa. The experimental data are taken from Ref. [22].

From Table 1, we can clearly see that for light and medium nuclei, the proton microscopic optical potential based on Skyrme force parameters SKa, SKb and SGI can reproduce the experimental data. From Table 1 the $\chi^2$ for $_{90}$Th for all microscopic optical potentials are very large. Among these 14 sets of Skyrme force parameters for proton microscopic optical potentials, the $\chi^2_{n\mathrm{SGI}}$, $\chi^2_{n\mathrm{SKa}}$ and $\chi^2_{n\mathrm{SKb}}$ have minimum values, which are basically close to the $\chi^2_{n\mathrm{CH89}}$ for almost all target nuclei.

Generally speaking, the $\chi^2_{ni}$ for $i$ = Ch89, KD, SGI, SKa and SKb are with small values and close to each other for all the 52 elements, and the values of $\chi^2_{ni}$ for $i$ = GS1-6, SBJS, SKM, SG Ⅱ, SG0 Ⅰ-Ⅱ are much larger than those of Ch89, KD, SGI, SKa and SKb for most of the 52 elements. From Table 4 we can clearly see that for both $\bar{\chi^2_i}$ and $\langle\bar{\chi^2}_i\rangle$, SGI, SKa and SKb have nearly equal small values which are close to those of KD and CH89, and the values of the others are much larger than those of CH89, KD, SGI, SKa and SKb. Therefore, we can conclude that the nucleon microscopic optical potentials with Skyrme force parameters GS1-6, SBJS, SKM, SG Ⅱ, SG0I-Ⅱ

are not suitable for calculating the proton optical potential. Also SGI, SKa and SKb are the three sets of best Skyrme force parameters for the proton microscopic optical potentials. These three sets of Skyrme force parameters are given in Table 5.

For giving an intuitive display, as examples we plot the experimental data and the theoretical values of the elastic scattering angular distributions for the target $^{24}$Mg in Fig. 1; and the reaction cross sections for the target element of Sn in Fig. 2. The theoretical values are calculated for the global proton optical potential obtained by Varner et al[6] in 1991 and one set of the proton microscopic optical potentials with modified Skyrme force parameters SKa[13]. From Fig. 1, except for some incident energies, the calculated values for the two sets of proton optical potentials basically reproduce the experimental data. From Fig. 2, we can see that the reaction cross sections for element Sn calculated using two sets of proton optical potentials reproduce the experimental data excellently.

## 4 Summary

In this work, for 112 target nuclei with proton as projectile, we compare the $\chi^2_{ni}$, $\bar{\chi^2_i}$ and $\langle\bar{\chi^2}_i\rangle$ values for 16 kinds of proton optical model potentials: two sets of phenomenological global optical potential[6, 7] and microscopic optical potentials[8] with 14 sets of Skyrme force parameters GS1-6[9], SBJS[10], SKM[11], SGI-Ⅱ[12], SKa-b[13], and SG0I-Ⅱ[14].

For giving an intuitive display, we plot the experimental data and the theoretical values of the elastic scattering angular distributions of the target $^{24}$Mg and the reaction cross sections of element Sn for two sets of proton optical potentials.

We find that for getting proton optical potentials, the nucleon microscopic optical potential[8] with Skyrme force parameters SGI, SKa and SKb are the three best sets because they can reproduce well the experimental data similar to the phenomenological global proton optical potentials CH89 and KD. These three sets of Skyrme force parameters are given in Table 5. Shen and co-workers[15—20] pointed out that for neutron as projectile, GS2 and SKa are the best two Skyrme force parameters for obtaining the microscopic nucleon optical potential. For deuteron as projectile, we constructed the deuteron optical potential with a folding model based on phenomenological and microscopic nucleon optical potentials[21], and found that SKa and SKb are the best two sets of Skyrme force parameters for constructing the deuteron optical potential based on s folding model. Therefore, we conclude that SKa is the common optimal set of Skyrme force parameters for obtaining the nucleon microscopic optical potential for proton, neutron and deuteron as projectile. The nucleon microscopic optical potential has a reliable theoretical basis; we can use it to predict the data of cross sections and angular distributions for those nuclei which lack experimental data and are outside the applicable nuclear ranges of the global phenomenological optical potential.

## References


1 Yong P G. RIPL Handbook, Vol. 41, 1998, http://www-nds.iaea.org/ripl/ (Chapter 4: Optical Model Parameters)
2 Jeukenne J P, Lejeune A, Mahaux C. Phys. Rev. C, 1977, **16**: 80
3 Brieva F A, Rook J R. Nucl. Phys. A, 1977, **291**: 317
4 Vinh Mau N, Bouyssy A. Nucl. Phys. A, 1976, **257**: 189
5 Bernard V, Van Giai N. Nucl. Phys. A, 1979, **327**: 397
6 Varner R L, Thompson W J, Mcabee T L, Ludwig E J, Clegg T B. Phys. Rep., 1991, **201**: 57
7 Koning A J, Delaroche J P. Nucl. Phys. A, 2003, **713**: 231
8 SHEN Qing-Biao, ZHANG Jing-Shang, TIAN Ye et al. Z. Phys. A, 1981, **303**: 69
9 Krewald S, Klemt V, Faessler A. Nucl. Phys. A, 1977, **281**: 166
10 Backman S O, Jackson A D, Speth J. Phys. Lett. B, 1975, **56**: 209
11 Kohler H, Treiner J, Bohigas O. Nucl. Phys. A, 1980, **336**: 155
12 Giai N V, Sagawa H. Phys. Lett. B, 1981, **106**: 379
13 Kohler H S. Nucl. Phys. A, 1976, **258**: 301
14 Treiner J, Krivine H. J. Phys. G, 1976, **2**: 285
15 CAI Chong-Hai, SHEN Qing-Biao, ZHUO Yi-Zhong. Nucl. Sci. Eng., 1991, **109**: 142
16 TIAN Ye et al. Chinese J. Nucl. Phys., 1985 **7**: 154
17 TIAN Ye et al. Chinese J. Nucl. Phys., 1985 **7**: 207
18 TIAN Ye et al. Chinese J. Nucl. Phys., 1985 **7**: 344
19 TIAN Ye et al. Chinese J. Nucl. Phys., 1986 **8**: 28
20 TIAN Ye et al. Chinese J. Nucl. Phys., 1988 **10**: 183
21 LI Xiao-Hua, AN Hai-Xia, CAI Chong-Hai. J. Eurp. Phys. A, 2009, **39**: 255
22 LI Xiao-Hua, CAI Chong-Hai. Nucl. Phys. A, 2008, **801**: 43
23 AN Hai-Xia, CAI Chong-Hai. Phys. Rev. C, 2006, **73**: 054605
24 Negele J W. Phys. Rev. C, 1970, **1**: 1260